BJP BRITISH JOURNAL OF PHARMACOLOGY

BPS BRITISH PHARMACOLOGICAL SOCIETY

British Journal of Pharmacology (2010), 160, 987–997

0007-1188/10
www.brjpharmacol.org

RESEARCH PAPER

Purinoreceptor-mediated current in myocytes from renal resistance arteries

Maksym I Harhun[1], Oleksandr V Povstyan[1,2] and Dmitri V Gordienko[1,2]

[1]*Ion Channels and Cell Signalling Centre, Division of Basic Medical Sciences, St. George's University of London, London, UK, and* [2]*Laboratory of Molecular Pharmacology and Biophysics of Cell Signalling, Bogomoletz Institute of Physiology, Kyiv, Ukraine*

Background and purpose: Ionotropic purinoreceptors (P2X) in renal vascular smooth muscle cells (RVSMCs) are involved in mediating the sympathetic control and paracrine regulation of renal blood flow (RBF). Activation of P2X receptors elevates $[Ca^{2+}]_i$ in RVSMCs triggering their contraction, leading to renal vasoconstriction and decrease of RBF. The goal of the present work was to characterize the P2X receptor-mediated ionic current (I_{P2X}) and to identify the types of P2X receptors expressed in myocytes isolated from interlobar and arcuate arteries of rat kidney.
Experimental approach: The expression of P2X receptors in isolated RVSMCs was analysed by reverse transcription (RT)–PCR. I_{P2X} and membrane potential were recorded using the amphotericin B-perforated patch method.
Key results: RT–PCR analysis on single RVSMCs showed the presence of genes encoding P2X1 and P2X4 receptors. Under voltage clamp conditions, the selective P2X receptor agonist αβ-methylene ATP (αβ-meATP) evoked I_{P2X} similar to that induced by ATP. Under current clamp conditions, both ATP and αβ-meATP evoked a spike-like membrane depolarization followed by a sustained depolarization, linking P2X receptors in RVSMCs to sympathetic control of renal vascular tone. A selective antagonist of P2X1 receptors, NF279, reduced I_{P2X} amplitude by ~65% concentration-dependently manner within the nanomolar to sub-micromolar range. The residual current was resistant to micromolar concentrations of NF279, but was inhibited by sub-millimolar to millimolar concentrations of NF279.
Conclusions and implications: Two types of functional P2X receptors, monomeric P2X1 and heteromeric P2X1/4 receptors, are expressed in RVSMCs. Our study has identified important targets for possible pharmacological intervention in the sympathetic control of renal circulation.
British Journal of Pharmacology (2010) **160,** 987–997; 10.1111/j.1476-5381.2010.00714.x

Keywords: renal vascular smooth muscle cells; kidney; artery; αβ-meATP; ATP; NF279; P2X1 receptors; P2X4 receptors; heteromeric P2X1/4 receptors

Abbreviations: αβ-meATP, αβ-methylene-adenosine 5′-triphosphate; GFR, glomerular filtration rate; NF279, 8,8′-(carbonylbis(imino-4,1-phenylenecarbonylimino-4,1-phenylenecarbonyl-imino)) bis(1,3,5-naphthalene-trisulphonic acid); NF449, 4,4′,4″,4‴-(carbonylbis (imino-5,1,3-benzenetriylbis-(carbonylimino))) tetrakisbenzene-1,3-disulphonic acid; RBF, renal blood flow; RSNA, renal sympathetic nerve activity; RT–PCR, reverse transcription–PCR; RVSMC, renal vascular smooth muscle cell; SM-MHC, smooth muscle myosin heavy chain

Introduction

Vascular smooth muscle tone is primarily regulated by the level of the intracellular Ca^{2+}: increased intracellular Ca^{2+} concentration ($[Ca^{2+}]_i$) leads to calmodulin-dependent phosphorylation of the myosin light chain, and thus, the development of force and contraction of the myocyte (Walsh, 1994). Two major co-transmitters ATP and noradrenaline contribute to the sympathetically mediated vasoconstriction of small arteries (Wier *et al.*, 2009). Ionotropic purinoreceptors (P2X) (nomenclature follows Alexander *et al.*, 2009) for ATP are ligand-gated cation channels, widely expressed in vasculature (Ralevic, 2009). Their activation following sympathetic nerve stimulation or selective agonist application leads to vasoconstriction, reduction of blood flow and an increase in blood pressure (Ralevic and Burnstock, 1991).

In the kidney, apart from being released as a co-transmitter from sympathetic nerve terminals, ATP is released by apical macula densa cells in response to an increase of NaCl

Correspondence: Dr Maksym Harhun, Ion Channels and Cell Signalling Centre, Division of Basic Medical Sciences, St. George's University of London, Cranmer Terrace, London, SW17 0RE, UK. E-mail: m.harhun@sgul.ac.uk
Received 12 November 2009; revised 31 December 2009; accepted 2 February 2010

concentration in the distal tubular fluid (Bell *et al*., 2003; Komlosi *et al*., 2006). An increase of ATP concentration in renal cortical interstitial fluid (Nishiyama *et al*., 2000; 2001), in turn, triggers P2X receptor-mediated vasoconstriction of afferent arterioles (Inscho *et al*., 2003) and, as a result, a decrease in renal blood flow (RBF) and glomerular filtration rate (GFR). This tubuloglomerular feedback mechanism (Nishiyama *et al*., 2000; Nishiyama and Navar, 2002; Guan *et al*., 2007a,b; Surprenant and North, 2009) and myogenic mechanism are two important components of renal autoregulation: an ability of the kidney to maintain a relatively constant RBF and GFR despite fluctuations in arterial pressure (Cupples and Braam, 2007). The faster myogenic mechanism (the inherent ability of vascular myocytes to adjust vascular diameter by rapid adjustment in tension in response to changes in transmural pressure) is crucial for protecting renal glomeruli from rapid elevations in arterial pressure (Cupples and Braam, 2007) and is considered to be the major contributor to autoregulatory resistance adjustments of the afferent arteriole and upstream arterial segments (Guan *et al*., 2007a). The slower tubuloglomerular feedback mechanism provides the means for the fine control of glomerular haemodynamics by regulating terminal arteriolar resistance (Cupples and Braam, 2007; Guan *et al*., 2007a).

From the therapeutic point of view, the importance of P2X receptors is in mediating of substantial vasoconstrictor drive which is resistant to adrenoceptor antagonists and calcium channel blockers (Evans and Surprenant, 1992; Bao and Stjarne, 1993; Galligan *et al*., 1995). Therefore, identification of the P2X receptor types expressed in smooth muscle cells of the resistance blood vessels and analysis of their pharmacological properties are a basis for the development of new specific therapies for the treatment of hypertension and other pathological conditions induced by elevated vascular tone.

Since the discovery of purinergic neurotransmission by Burnstock (1972), seven subunits of the P2X receptor family have been identified (P2X1–P2X7), each of them coded by a distinct gene (North, 2002). These subunits can be assembled in various configurations to form homomeric or heteromeric channels (Torres *et al*., 1999). The functional P2X receptors are likely to be composed of three subunits (North and Verkhratsky, 2006). While the distribution and properties of P2X receptors in the nervous system have been extensively studied (North, 2002; North and Verkhratsky, 2006), only a few studies have analysed the pharmacological properties of the P2X receptor-mediated current in vascular smooth muscle cells (Evans and Surprenant, 1992; Loirand and Pacaud, 1995; Cario-Toumaniantz *et al*., 1998; Lewis and Evans, 2000). Many studies of P2X receptors in vasculature are limited to the immunohistochemical identification of the P2X receptor protein distribution in the vascular wall (Chan *et al*., 1998; Lewis and Evans, 2001; Turner *et al*., 2003), which does not allow for the detection of the heteromeric P2X receptors and does not elucidate the pharmacological properties of endogenous P2X receptors expressed in vascular smooth muscle cells.

The expression of P2X receptors in renal vasculature has been identified mostly using immunohistochemical labelling. In this way, the P2X1 receptor was detected in pre-glomerular arteries and afferent arterioles (Chan *et al*., 1998; Lewis and Evans, 2001; Turner *et al*., 2003), while P2X2 and P2X5 were barely detected in small arteries (Lewis and Evans, 2001), and P2X4 and P2X7 receptors were detected in small and medium arteries (Lewis and Evans, 2001). To our knowledge, there is no study on renal vascular smooth muscle cells (RVSMCs) in which the expression of the genes for functional P2X receptors and the pharmacological properties of P2X receptor-mediated ionic current were examined. Therefore, in this study, we focused on the analysis of the expression of the genes encoding P2X receptors in single smooth muscle cells freshly isolated from interlobar and arcuate arteries of rat kidney and of pharmacological and biophysical properties of the P2X receptor-mediated ionic currents in these myocytes. A preliminary account of this study was previously published in abstract form (Harhun *et al*., 2009)

Methods

Cell Preparation

All animal care and experimental procedures were in accordance with the UK Animals Scientific Procedures Act 1986. Interlobar and arcuate arteries were microdissected from rat kidney as previously described (Gordienko *et al*., 1994). Male Wistar Kyoto rats (180–250 g, 35 animals obtained from Charles Rivers laboratories, Margate, UK) were humanely killed by cervical dislocation followed by exsanguination. Following the dissection, the vessels were cleaned of adherent connective tissues. Single RVSMCs were obtained by enzymatic dispersion (Harhun *et al*., 2004; 2006) and allowed to settle down in experimental chambers in physiological saline solution (PSS, in $mmol \cdot L^{-1}$: KCl, 6; NaCl, 120; $MgCl_2$, 1.2; $CaCl_2$, 1.0; D-glucose, 10; and HEPES, 10; pH was adjusted to 7.3 with NaOH). RVSMCs then were either collected for reverse transcription (RT)–PCR experiments or used in patch clamp experiments within 6 h of isolation.

RT–PCR analysis

For the RT–PCR, single RVSMCs (pool of ~500 cells per sample) were collected under the microscope (Axiovert 100M, Carl Zeiss Ltd, Oberkochen, Germany) using a wide-bore glass micropipette pipette attached to a micromanipulator and frozen on dry ice immediately after collection. Total RNA was extracted using the Qiagen RNeasy extraction kit (Qiagen, Crawley, UK). cDNA was obtained using Superscript II Reverse Transcriptase (Invitrogen, Paisley, UK) and used in PCR. cDNA was used as a template in a 50 mL PCR reaction containing 1.5 $mmol \cdot L^{-1}$ $MgCl_2$, 0.2 $mmol \cdot L^{-1}$ deoxynucleoside triphosphates, 0.2 $mmol \cdot L^{-1}$ forward and reverse primers (Invitrogen) and 2.5 units of platinum *Taq* DNA polymerase (Invitrogen). Amplification was performed according to the following schedule using a Techne Thermocycler (Bibby Scientific Ltd, Stone, UK): 94°C for 2 min; 40 cycles of 94°C for 30 s; 57°C for 60 s; and 72°C for 3 min, followed by a final elongation period of 10 min at 72°C. No-template control PCR was also performed simultaneously with every reaction. Primers were designed so that they spanned at least one intron of the genomic sequence to avoid detecting genomic DNA contamination. The experiments were repeated four times with

samples of RVSMCs from different animals. The primers were designed to amplify the genes encoding proteins of interest. The purity of the sample of RVSMCs collected for RT–PCR analysis was confirmed by the expression of the gene encoding the smooth muscle cell marker, smooth muscle myosin heavy chain (SM-MHC), but not the markers for other cell types present in the vascular wall such as: fibroblasts and endothelial cells (CD34), neurons (PGP9.5) and pericytes (NG2). The PCR products were separated and visualized in ethidium bromide-stained 2% agarose gel by electrophoresis.

The following primers were used in these experiments (the following data are shown in brackets: GeneBank accession number, the sense bordering nucleotide position and the antisense bordering nucleotide position): β-actin (NM_031144, 306-325 and 1007-1026), SM-MHC for SMCs (Yoshida and Owens, 2005) (X16262, 447-466 and 1182-1191), CD34 for endothelial cells and fibroblasts (Vanderwinden *et al*., 1999) (XM_223083, 218-237 and 1050-1069), PGP9.5 for neurons (Wilkinson *et al*., 1989) (D10699, 54-73 and 544-563), NG2 proteoglycan for pericytes (Hughes and Chan-Ling, 2004) (NM_031022, 1815-1834 and 2791-2810), P2X1 receptor (NM_012997, 309-328 and 1119-1138), P2X2 (NM_053656, 603-622 and 1590-1609) P2X3 (NM_031075, 217-236 and 1215-1234), P2X4 (NM_031594, 356-375 and 1061-1080), P2X5 (NM_080780, 360-379 and 1335-1354) and P2X7 (NM_019256, 610-629 and 1563-1582).

Electrophysiological recordings

Electrical recordings were made in PSS using the amphotericin B-perforated patch tight-seal whole-cell recording technique in voltage clamp or current clamp modes. The fire-polished patch pipettes had a free-tip resistance of 4–5 MOhm when filled with pipette solution of the following composition ($mmol \cdot L^{-1}$): KCl, 115; NaCl, 6; HEPES, 10; pH adjusted to 7.3 with KOH. Prior to the experiment, the pipette solution was supplemented with amphotericin B (200 $mg \cdot mL^{-1}$). When the properties of I_{P2X} were examined (Figures 3–6), to eliminate the possible contribution of the current through potassium channels to the whole-cell current records, K^+ was equimolarly replaced with Cs^+ in both external and pipette solutions. ATP and αβ-meATP were applied by 2 s pulses through a glass micropipette (located within 100 μm of the cell surface) connected to a pressure ejector PicoSpritzer III (Intracel, Shepreth, UK). The electrical signals were recorded using an Axopatch 200A patch clamp amplifier (Axon Instruments, Foster City, CA, USA). Electrical signals were generated and digitized at 1 kHz using a Digidata 1200 hosted by a PC running pClamp 6.0 software (Axon Instruments). Voltage clamp experiments were carried out at a holding potential of –60 mV at room temperature (21–24°C). Data were analysed and plotted using MicroCal Origin and CorelDraw software.

Statistical analysis

All data are presented as mean ± SEM with the number of cells shown for data points obtained from at least three animals. Comparative analysis of the data was performed using the Student's *t*-test.

Materials

The RNA extraction kit was purchased from Qiagen; the primers and other reagents for RT–PCR experiments were purchased from Invitrogen. The rest of the reagents were purchased from Sigma-Aldrich (Poole,UK) with the exception of NF279 and NF449 which were purchased from Tocris (Bristol, UK).

Results

Isolated RVSMs express genes encoding P2X1 and P2X4 receptors

To determine the expression of genes encoding P2X receptor subunits in RVSMCs, the RT–PCR experiments were performed on cDNA obtained from single isolated myocytes (~500 cells for each RT–PCR run) manually collected under the microscope. Even though only those cells with a distinct smooth muscle cell morphology were collected in these experiments, to ensure the purity of each sample, the preparations were tested for the presence of the smooth muscle cell marker, as well as for the markers for other cell types which normally occur in the blood vessel wall, such as fibroblasts, endothelial cells, neurons and pericytes (see Methods). Only those preparations, which showed the expression of the gene encoding SM-MHC (a smooth muscle cell marker), but not the markers for other cell types (Figure 1A) were used for detection of the expression of genes encoding P2X receptor proteins: P2X1–P2X5 and P2X7. As several previous studies on immunodetection of P2X receptor proteins demonstrated that the P2X6 receptor is not expressed in renal vasculature (Lewis and Evans, 2001; Guan *et al*., 2007a,b), the expression of the gene encoding this protein was excluded from the analysis. We found that RVSMCs express genes encoding P2X1 and P2X4 receptors, but not P2X2, P2X3, P2X5 or P2X7 receptor proteins (Figure 1B).

ATP and αβ-meATP evoke similar electrical events in RVSMCs

In PSS under whole-cell voltage clamp conditions at a holding potential of –60 mV, a 2 s application of 10 μM ATP evoked a rapidly activating inward current with an average peak current density of 82 ± 8 $pA \cdot pF^{-1}$ (n = 7). After reaching the peak, the current started to desensitize before termination of the drug application (Figure 2Aa). Under current clamp conditions, the application of ATP evoked a biphasic depolarization: (i) an initial spike-like depolarization was followed by (ii) a sustained component during which the cell membrane potential slowly recovered towards the resting level (Figure 2Ab). To test whether these ATP-evoked electrical events were mediated by P2X receptors, the action of a potent selective P2X receptor agonist, αβ-meATP (Bo and Burnstock, 1995) on the whole-cell membrane current, and membrane potential was examined and compared with that of ATP. Under the same experimental conditions, application of 10 μM αβ-meATP evoked an inward current with similar kinetics and peak amplitude (mean peak current density of 112 ± 27 $pA \cdot pF^{-1}$, n = 5) (Figure 2Ba) and similar biphasic changes in the RVSMC membrane potential (Figure 2Bb) as ATP. These data strongly suggest that the ATP-evoked inward

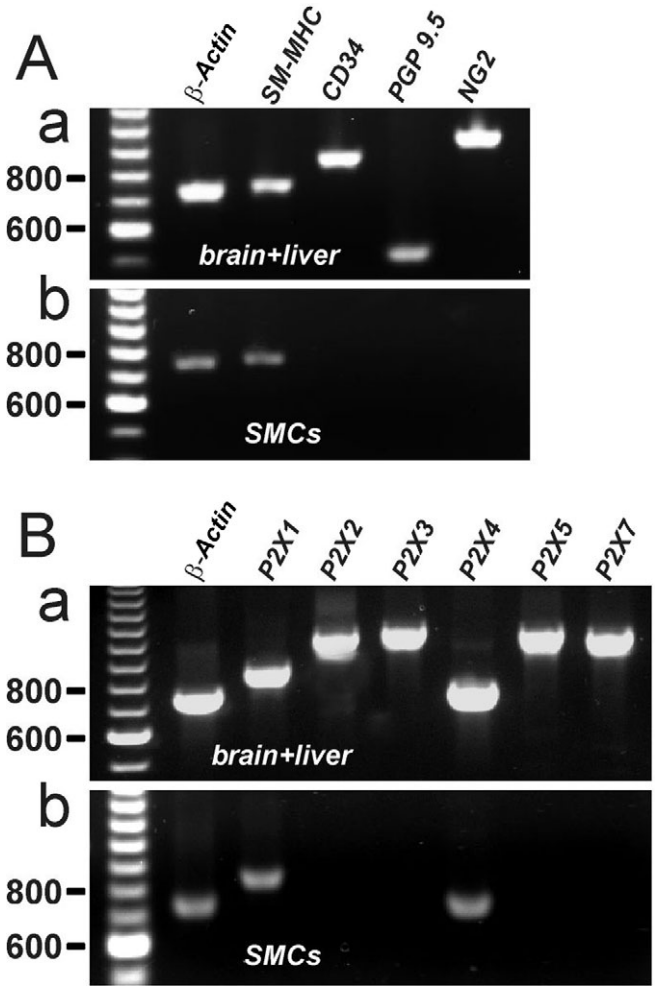

Figure 1 RT–PCR analysis of P2X receptor expression in RVSMCs from rat renal resistance arteries. (A) The purity of the preparation was verified using primers designed to amplify genes encoding the markers for certain cell types which can be found in blood vessel: SM-MHC (745 bp) for smooth muscle cells, CD34 (852 bp) for fibroblasts and endothelial cells, PGP9.5 (510 bp) for neurons, NG2 (996 bp) for pericytes. As a positive control, primers for β-actin (721 bp) were used. Primers were tested for their specificity using cDNA preparations from a mixture of rat brain and liver tissue (Aa). The RVSMCs preparation showed expression of genes encoding β-actin and SM-MHC only. (Ab). (B) Primers designed to amplify genes encoding P2X receptors sub-types: P2X1 (830 bp), P2X2 (1007 bp), P2X3 (1018), P2X4 (725 bp), P2X5 (995 bp) and P2X7 (973 bp) were tested for their specificity using cDNA preparations of rat brain and liver tissue (Ba) before using them with SMCs preparations (Bb). RVSMCs were found to express genes encoding only two types of P2X receptor proteins: P2X1 and P2X4.

current is mediated by P2X receptors and that activation of this current induces depolarization of the RVSMC membrane. On a number of occasions, the 'outburst' of outward current was observed within 5 s after the peak of the inward current (data not shown).

Properties of I_{P2X} in RVSMCs

Taking into account that activation of P2X receptors by either ATP or αβ-meATP led to an abrupt increase of $[Ca^{2+}]_i$ in RVSMCs (Harhun *et al*., 2009), this outward current, as well as spontaneous transient hyperpolarizations observed in the background of the sustained membrane depolarization (Figure 2Bb) may result from the burst opening of clusters of high-conductance Ca^2 ± dependent K^+ channels (Benham *et al*., 1986; Stehno-Bittel and Sturek, 1992). Therefore, in all subsequent experiments, where the properties of P2X receptor-mediated current were analysed, to eliminate the contribution of potassium channel-mediated current to the whole-cell current, K^+ was replaced by Cs^+ in both external and pipette solutions. Under these conditions, a 2 s application of 10 μM ATP evoked an inward current with an average peak current density of 86 ± 14 pA·pF^{-1} (n = 7) (Figure 3A). The current reached its peak within 30–200 ms, and then decayed before termination of the drug application. Application of 10 μM αβ-meATP evoked a similar inward current with an average peak current density of 111 ± 5 pA·pF^{-1} (n = 123; the electrical capacitance of the cell membrane was on average 19.0 ± 0.4 pF). Application of 10 μM UTP, which has been reported to be less potent at P2X1 receptors than ATP in rat tail artery myocytes (McLaren *et al*., 1998), evoked significantly smaller currents (Figure 3A) with an average peak current density of 3 ± 2 pA·pF^{-1} (n = 7) in RVSMCs. Because αβ-meATP is a more selective agonist of P2X receptors than ATP (Gerdes *et al*., 1991), we used this compound to activate I_{P2X} in all subsequent experiments.

To confirm further that the αβ-meATP-evoked inward current is mediated by P2X1 receptors, the action of the potent selective P2X1 receptor antagonists NF279 (Damer *et al*., 1998; Rettinger *et al*., 2000) and NF449 (Rettinger *et al*., 2005) on I_{P2X} was tested (Figure 3Ba). Then, 2 nM of NF279 inhibited I_{P2X} by about 20% (n = 5), whereas the same concentration of NF449 suppressed I_{P2X} more strongly, by about 60% (n = 7) (Figure 3Bb). These data are consistent with the higher potency of NF449 at P2X1 receptors (reported IC_{50} is 19 and 0.05 nM for NF279 and NF449, respectively) (Rettinger *et al*., 2000; Hulsmann *et al*., 2003). However, 2 nM of NF449 almost completely abolished the current mediated by recombinant P2X1 receptors (Hulsmann *et al*., 2003), but reduced I_{P2X} in RVSMCs only by ~60%. This discrepancy suggests the contribution of other than P2X1 receptor to αβ-meATP-evoked I_{P2X} in RVSMCs.

To study the recovery of I_{P2X} from desensitisation, 2 s pulses of 10 μM αβ-meATP were applied repetitively with gradually increasing intervals (Figure 4Aa). This approach revealed that a 7 min interval between subsequent applications of αβ-meATP was required for almost complete recovery of I_{P2X} (n = 6; Figure 4Ab). Therefore, in all subsequent experiments, the 2 s pulses of αβ-meATP were applied with an interval of 7–8 min to allow for the P2X receptor re-sensitization. The rate of the I_{P2X} desensitization, as well as the relative contribution of the slow (sustained) component of the current varied from cell to cell and even in the same RVSMC upon repetitive applications of αβ-meATP (Figure 4Aa, pointed out by arrows). This variability precluded accurate analysis of these parameters.

To study the voltage–dependence of I_{P2X}, the 2 s pulses of 10 μM αβ-meATP were applied at different holding potentials: between –60 and +20 mV in 20 mV increments (Figure 4Ba). The current–voltage relationship for the peak I_{P2X}

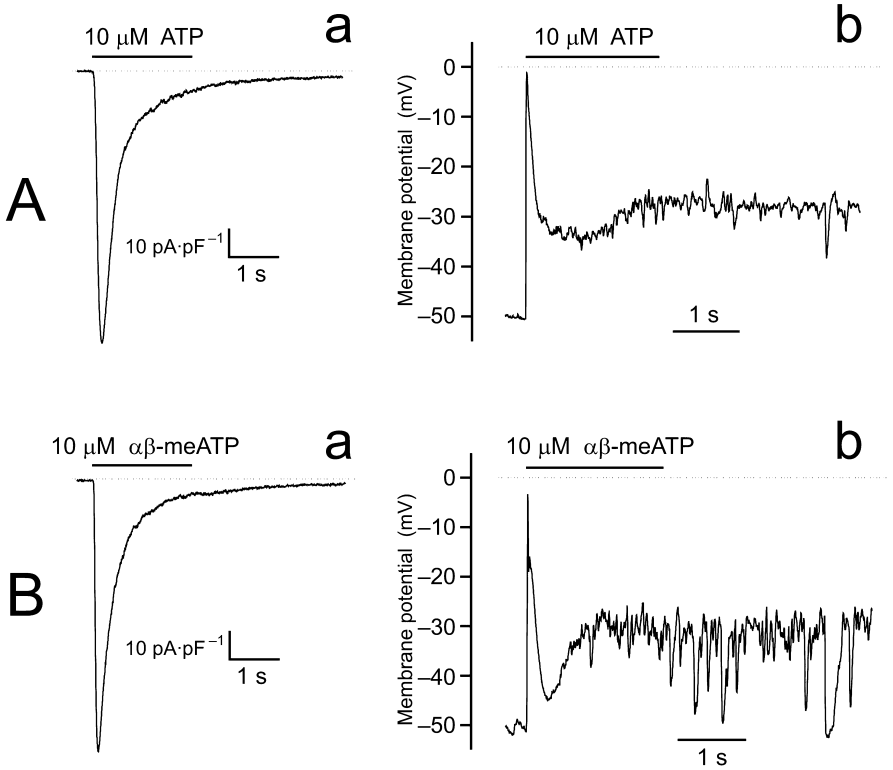

Figure 2 Electrical events induced by ATP and αβ-meATP in RVSMCs. 2 s pulses of ATP (10 μM) or selective P2X receptor agonist αβ-meATP (10 μM) evoked similar inward currents (Aa and Ba correspondingly) or changes of the cell membrane potential (Ab and Bb, respectively) suggesting a crucial role of P2X receptors in mediating the response of RVSMCs to ATP.

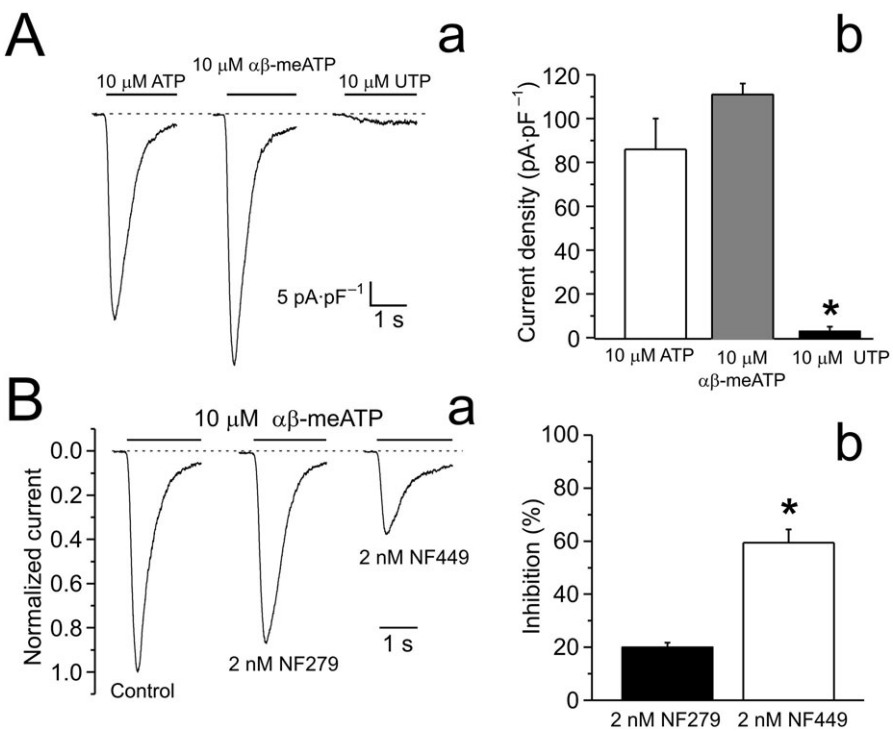

Figure 3 (Aa) Traces of the inward current elicited in RVSMCs by 10 μM ATP, 10 μM αβ-meATP and 10 μM UTP at holding potential −60 mV. (Ab) The peak current density for I_{P2X} induced by 10 μM of ATP ($n = 7$), 10 μM of αβ-meATP ($n = 123$) and 10 μM of UTP ($n = 7$). (Ba) Action of NF279 and NF449 on the inward current activated by 10 μM αβ-meATP. (Bb) Inhibition of I_{P2X} by 2 nM NF279 ($n = 5$) and 2 nM NF449 ($n = 7$). * indicates $P < 0.05$.

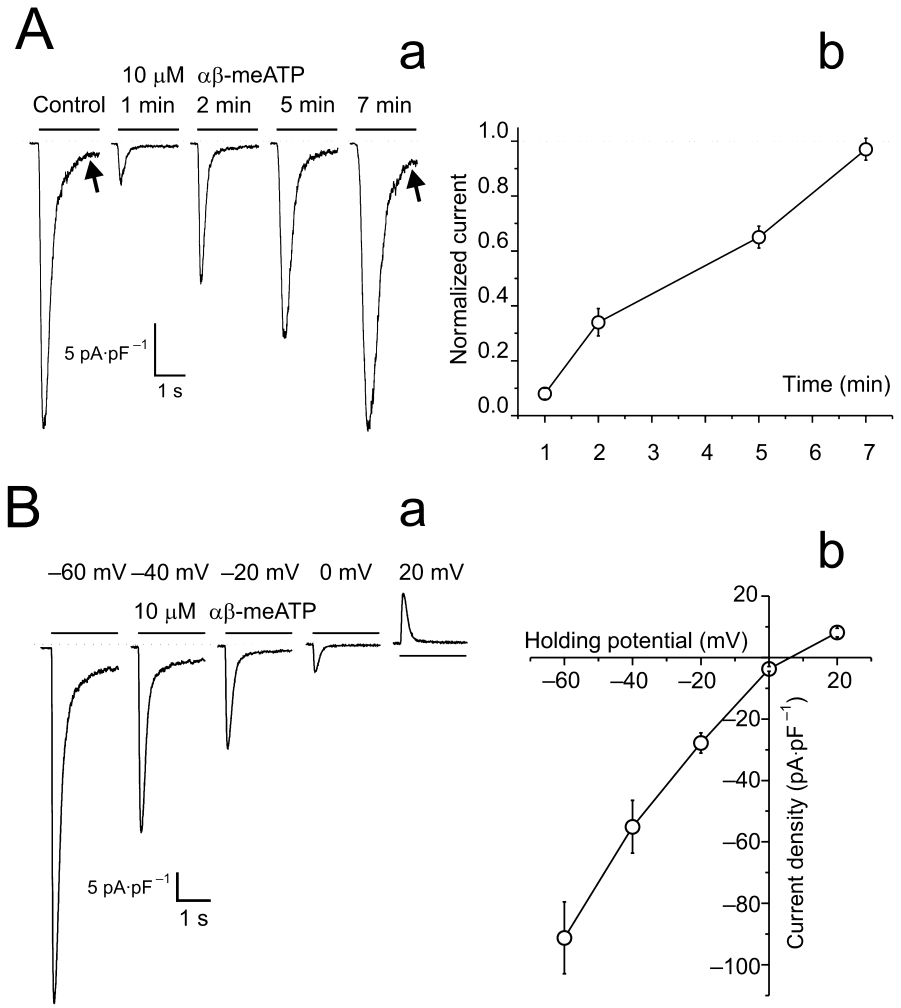

Figure 4 (A) Kinetics of re-sensitization of P2X receptors in RVSMCs. (Aa) The 2 s pulses of 10 μM αβ-meATP were repetitively applied with different intervals, as indicated. Virtually complete recovery of the peak current density was observed within 7 min. Representative traces recorded in single cell illustrate some variability in the relative contribution of the sustained component to I_{P2X} (arrows). (Ab) Averaged time-course of I_{P2X} re-sensitization: the averaged peak current densities were normalized to the peak current density induced by the first αβ-meATP application and plotted versus duration of intervals between subsequent αβ-meATP applications (n = 6–7 cell for each point). (B) Voltage–dependence of I_{P2X}. (Ba) Representative current traces recorded in single RVSMC. (Bb) Current–voltage relationship for the peak I_{P2X} revealed inward rectification (n = 5).

obtained in this way, revealed inward rectification and a reversal potential around +5 mV (Figure 4Bb), which is consistent with characteristics of the P2X receptor-mediated cationic current in other preparations (North, 2002).

Within the range of concentrations between 10 nM and 100 μM, αβ-meATP activated I_{P2X} concentration dependently with an EC_{50} of 1.1 ± 0.1 μM (n = 5–6 for different concentrations of αβ-meATP) (Figure 5A). The rate of both activation and desensitization of I_{P2X} increased with increasing concentration of αβ-meATP (Figure 5Aa). The time to peak of I_{P2X} activated by 10 nM of αβ-meATP (990 ± 17 ms; n = 5) was more then 10 times that of I_{P2X} activated by 10 μM αβ-meATP (85 ± 22 ms; n = 5). The kinetics of I_{P2X} and its affinity to αβ-meATP (EC_{50} of around 1 μM) are consistent with characteristics of the cationic current mediated by cloned P2X1 receptors (Rettinger *et al*., 2000). We therefore concluded that monomeric P2X1 receptors make the predominant contribution to the genesis of I_{P2X} in RVSMCs.

The I_{P2X} evoked by 10 μM of αβ-meATP was attenuated by gradually increasing extracellular Ca^{2+} concentration, $[Ca^{2+}]_o$ (Figure 5B), with no apparent changes in the kinetics of the current. An increase in extracellular Ca^{2+} from 1 to 5 mM reduced the peak current density by 33 ± 7% (n = 6–7 for different $[Ca^{2+}]_o$). The decrease of $[Ca^{2+}]_o$ from 1 mM to 10 μM resulted in an increase of the peak current density by 70 ± 15%. This property of the cationic current mediated through endogenous P2X receptors in RVSMC differs from that of the current mediated by cloned P2X1 receptors, which was reported to show little if any dependence on $[Ca^{2+}]_o$ (Evans *et al*., 1996).

NF279 was reported to be a potent selective and reversible antagonist of the P2X1 receptors with ~15 000 times greater affinity for P2X1, than for P2X4, receptors (Damer *et al*., 1998; Rettinger *et al*., 2000). Because the RVSMCs showed the presence of mRNA only for these two types of P2X receptors, the effect of NF279 on I_{P2X} was studied. The results of these experi-

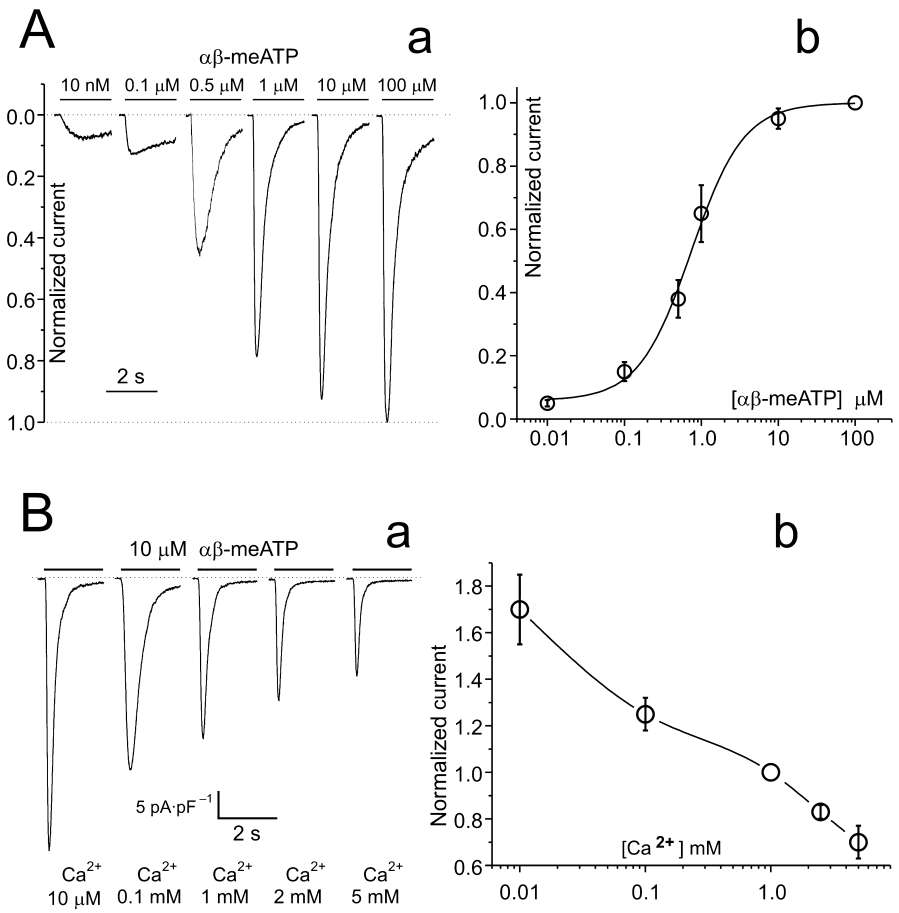

Figure 5 (A) Concentration–dependence of activation of I_{P2X} by αβ-meATP. (Ab) Traces of I_{P2X} evoked by various concentrations of αβ-meATP were normalized to the peak amplitude of the maximal response evoked by 100 μM of αβ-meATP. (Ab) Averaged normalized peak amplitude of I_{P2X} was plotted versus corresponding concentration of αβ-meATP (n = 5–6). The concentration–dependence curve fitted to the experimental points using non-linear least square minimization algorithm revealed an EC_{50} = 1.1 ± 0.1 μM. (B) Dependence of I_{P2X} on extracellular Ca^{2+} concentration ($[Ca^{2+}]_o$). (Ba) I_{P2X} was elicited by repetitive (with 8 min interval) applications of 10 μM αβ-meATP to RVSMC incubated in external solutions with gradually increasing $[Ca^{2+}]_o$, as indicated. (Bb) The plot of the dependence of I_{P2X} on $[Ca^{2+}]_o$ revealed that increase in $[Ca^{2+}]_o$ from 1 to 5 mM reduced I_{P2X} by 33 ± 7% (n = 5–6).

ments are summarized in Figure 6A. The original traces of I_{P2X} induced by a 2 s pulse of 10 mM αβ-meATP under control conditions and following 5 min incubation with different concentrations (from 10 nM to 2 mM) of NF279 are shown in Figure 6Aa. From these records, the values of the peak current density were calculated and plotted against the corresponding concentration of NF279. The concentration–response curve for the antagonistic effect of NF279 obtained in this way revealed an inflexion (Figure 6Ab), strongly suggesting the contribution of two types of functional P2X receptors with different affinities to NF279. The least square fit of the concentration–response curve(s) to the data revealed that the I_{P2X} component with higher sensitivity to NF279 was characterized by an IC_{50} = 6.8 ± 0.4 nM, while the component with lower sensitivity to NF279 was characterized by an IC_{50} = 71.4 ± 2.8 μM. The high sensitivity of the first component to NF279 is consistent with the high affinity of the cloned P2X1 receptor to this drug. The sensitivity of the second component was close to that reported for the cloned P2X3 receptor (Rettinger *et al.*, 2000). However, expression of the gene encoding the P2X3 receptor protein was not detected in RVSMCs (Figure 1B). In addition, the recovery from desensitization of I_{P2X} in RVSMCs was much slower than that reported previously for the current mediated by the P2X3 receptor (Rettinger *et al.*, 2000).

The P2X4 receptor is characterized by very low affinity for αβ-meATP, so that αβ-meATP is virtually incapable of activating any current through monomeric P2X4 receptors at concentrations below 100 μM (North, 2002). However, current responses to stimulation with αβ-meATP at concentrations below 100 μM have been obtained from *Xenopus* oocytes expressing the rat P2X4 receptor orthologue (Le *et al.*, 1998). The P2X4 receptor is also characterized by a low affinity to NF279, so that concentration–response curve for the antagonistic effect of NF279 on P2X4 receptor-mediated current gives an IC_{50} higher than 300 μM (Rettinger *et al.*, 2000). The P2X4 receptor-mediated current is also known to be potentiated by the antiparasitic agent, ivermectin (Khakh *et al.*, 1999). Following incubation with 2 μM NF279, the peak current density of I_{P2X} in RVSMCs was reduced to 38 ± 4% of its control value, while subsequent incubation of the myocytes with 3 μM ivermectin in the presence of 2 μM NF279

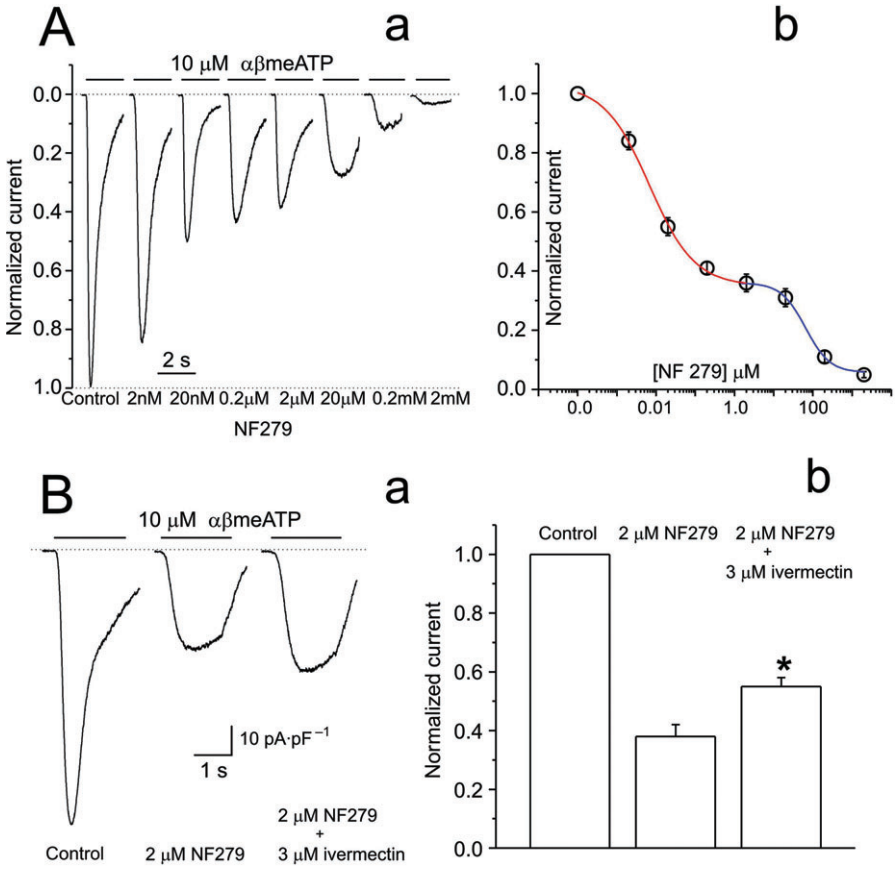

Figure 6 (A) Concentration–dependence of inhibition of I_{P2X} by NF279 (Aa) Traces of I_{P2X} evoked by repetitive (with 8 min interval) applications of αβ-meATP following 5 min pre-incubation with gradually increasing concentrations of NF279, as indicated. Currents were normalized to the peak amplitude of I_{P2X} recorded in the absence of NF279. (Ab) Averaged normalized peak amplitude of I_{P2X} was plotted versus corresponding concentration of NF279 (n = 5–12 for each data point). The best fit of the theoretical sigmoidal curves to the experimental points using a non-linear least square minimization algorithm resulted in two distinct sigmoid curves. Thus, two components with different sensitivity to NF279 contributed to I_{P2X}: the high-affinity component (with IC_{50} = 6.8 ± 0.4 nM, fitted by red sigmoid) and the low-affinity component (with IC_{50} = 71.4 ± 2.8 μM, fitted by blue sigmoid). (B) Potentiation of NF279-resistant I_{P2X} by ivermectin. (Ba) I_{P2X} persisting in the presence of 2 μM NF279 was augmented by 3 μM of ivermectin, a positive P2X receptor modulator. (Bb) Summary of the data obtained in five RVSMCs. For each cell, the peak current density detected in the presence of the drug or drug combination was normalized to that in control. NF279 (2 μM) reduced the peak current density relative to its control magnitude. Subsequent incubation with 3 μM ivermectin in the presence of 2 μM NF279 partly reversed the inhibition due to NF279. * indicates $P < 0.05$.

partly restored the peak current density to 55 ± 3% of its control magnitude (Figure 6B; n = 5).

Altogether, the results shown above strongly suggested that in RVSMCs, the P2X4 receptor protein is involved in the formation of a functional ligand-gated ion channel responsible for the genesis of the sustained component of I_{P2X}. As sensitivity of this component to both αβ-meATP and NF279 was higher than that previously reported for the monomeric P2X4 receptor (Rettinger *et al*., 2000; North, 2002), but was similar to that reported for the heteromeric P2X1/4 receptor (Nicke *et al*., 2005), we concluded that in RVSMCs P2X4 receptor subunits co-assemble with P2X1 receptor subunits to form functional heteromeric P2X1/4 receptors. The current through these heteromeric P2X1/4 receptors is known to have the kinetics of activation and desensitization slower than that of monomeric P2X1 receptor-mediated current (Nicke *et al*., 2005), and therefore may contribute to the sustained component of I_{P2X} in RVSMCs.

Discussion

This study demonstrates the expression of the genes encoding P2X1 and P2X4 receptor proteins in single smooth muscle cells freshly isolated from renal resistance arteries. The expression of the genes encoding these proteins was previously demonstrated in renal vasculature in experiments which were conducted on mutlicellular preparations such as blood vessel fragments (Chan *et al*., 1998; Nori *et al*., 1998; Lewis and Evans, 2001). In contrast to the previous experiments where the expression of P2X2, P2X3 and P2X7 receptors in the wall of renal resistance blood vessels was immunodetected (Lewis and Evans, 2001), we found no evidence for the expression of the genes encoding these proteins in single RVSMCs. The explanation for this discrepancy is that immunostaining of the blood vessel also involves staining cells other than RVSMC, such as endothelial cells, fibroblasts, neurons or pericytes, where P2X2, P2X3 and P2X7 receptors could be

expressed. We have conducted RT–PCR analysis on single isolated RVSMCs which were collected one by one under a high-resolution microscope using glass micropipettes. Furthermore, the purity of the smooth muscle cell sample was confirmed by the expression of the gene encoding a smooth muscle cell marker (SM-MHC), but not the markers for other cell types normally found in the vascular wall: fibroblasts and endothelial cells (CD34), neurons (PGP9.5) and pericytes (NG2). This approach ensures that the analysis of the expression of genes encoding P2X receptor subunits was restricted to RVSMCs.

Because the P2X-mediated current recorded under conventional whole-cell voltage clamp reveals a run-down (Lewis and Evans, 2000), to improve reproducibility of the αβ-meATP-induced I_{P2X} in RVSMCs, which is vital for adequate pharmacological experiments, the amphotericin B-perforated patch configuration of the whole-cell tight-seal recording was used in all our electrophysiological experiments. Under these conditions, 2 s pulses of 10 μM ATP evoked in RVSMCs a rapidly activating and desensitizing ionic current. The kinetics of this current and the peak current density were identical to that recorded in response to stimulation with the potent selective agonist of the P2X1 receptor αβ-meATP. The current induced by 10 μM αβ-meATP also desensitized rapidly in the presence of the agonist, and completely recovered from desensitization within 7 min. These characteristics of the I_{P2X} in RVSMCs, as well as its high sensitivity to αβ-meATP (EC_{50} = 1.1 μM), are similar to that previously reported for the recombinant P2X1 receptor (Valera *et al*., 1994; Evans *et al*., 1995). However, there were two major discrepancies between the characteristics of I_{P2X} in RVSMCs and that of recombinant P2X1 receptor-mediated current. First, there was a significant variability in the ratio of the sustained-to-peak-current amplitude was observed and, second, nanomolar concentrations of the selective P2X1 receptor antagonist, NF279, which are known to suppress the current through the recombinant P2X1 receptors completely (Rettinger *et al*., 2000), inhibited I_{P2X} in RVMSCs by only ~65%. Taking into account that mRNA for the P2X4 receptor protein was detected in RVSMCs, it is reasonable to assume that this P2X receptor type is mainly responsible for the genesis of the sustained component of I_{P2X} recorded in RVSMCs. The P2X4 receptor-mediated current is known to have a much slower rate of desensitization than the current mediated by P2X1 receptors (North, 2002). The variation in relative contribution of P2X1 and P2X4 receptors to I_{P2X} in RVSMCs may account for the variability in the ratio of the sustained-to-peak-current amplitude. However, αβ-meATP is a weak agonist of P2X4 receptors, virtually incapable of activating a measurable P2X4 receptor-mediated current at the concentrations (<100 μM) used in our experiments (Le *et al*., 1998; North, 2002). Nevertheless, in RVSMCs, the current resistant to nanomolar concentrations of NF279 accounted for about ~35% of the total I_{P2X}. Furthermore, recombinant P2X4 receptors are characterized by rather low affinity to NF279: IC_{50} > 300 μM (Rettinger *et al*., 2000). In contrast, in RVSMCs, the component of I_{P2X} with lesser sensitivity to NF279 was inhibited by micromolar concentrations of the antagonist with an IC_{50} of 71.4 μM. Thus, it is rather unlikely that monomeric P2X4 receptors make a significant contribution to the genesis of I_{P2X} in RVSMCs. It is possible, however, that the activation of monomeric P2X4 receptors was responsible for the genesis of a small fraction of the I_{P2X} which appeared to be insensitive to 2 mM of NF279. The absence of a current with evident P2X4 receptor properties could also be explained by either low expression of the corresponding subunit or inability of the subunits to form a functional channel. The properties of the I_{P2X} component resistant to nanomolar concentrations of NF279 therefore do not conform to the properties of the currents evoked by activation of either recombinant P2X1 or P2X4 receptors, the genes for which were found to be expressed in RVSMCs.

There are seven types of mammalian P2X receptor subunits (P2X1–P2X7), which can form homomeric ionic channels (North, 2002). Most of these subunit types have an ability to co-assemble with other types of P2X receptor subunits and form heteromeric channels with distinct pharmacological and biophysical properties (North, 2002). Earlier studies based on the results of co-immunoprecipitation of P2X receptor subunits suggested the potential co-assembly of different P2X receptors subunits (Torres *et al*., 1999). Interestingly, these studies have shown no potential co-assembly of P2X1 and P2X4 receptor subunits; the gene expression for which we identified in RVSMC. More recently, the biochemical and functional evidence for heteromeric assembly of P2X1 and P2X4 receptor subunits was reported (Nicke *et al*., 2005). In that study, it was demonstrated that the heteromeric P2X1/4 receptor-mediated current had kinetics of activation and desensitization slower than that of monomeric P2X1 receptor-mediated current and was activated by micromolar concentrations of αβ-meATP with an EC_{50} of 35.8 μM. Overall, the characteristics of the component of I_{P2X} resistant to nanomolar concentrations of NF279 recorded in our experiments were consistent with the properties of heteromeric P2X1/4 receptors (Nicke *et al*., 2005), suggesting a contribution of a heteromeric P2X1/4 receptors to the genesis of I_{P2X} in RVSMCs. The application of the P2X4 receptor agonist ivermectin evoked an increase of I_{P2X} persisting in micromolar concentrations of NF279. However, it is unclear whether this resulted from activation of heteromeric P2X1/4 receptors or monomeric P2X4 receptors, a small fraction of which could still be activated by 10 μM αβ-meATP (Le *et al*., 1998). Finally, variations in the relative contribution of the sustained component of the I_{P2X} elicited in the same RVSMC by repetitive applications of 10 μM αβ-meATP can also be explained by the low affinity of heteromeric P2X1/4 receptors for αβ-meATP. Indeed, 10 μM αβ-meATP caused nearly maximal activation of P2X1 receptors (reported $EC_{50} \approx 1$ μM; see also Figure 5A), but only slightly activated heteromeric P2X1/4 receptors (reported $EC_{50} \approx 35.8$ μM) (Nicke *et al*., 2005).

P2 receptors are expressed in renal vascular, glomerular, mesangial and tubular epithelial cells, implying that ATP is involved in a diverse array of physiological mechanisms regulating renal hemodynamics and tubular function (Guan *et al*., 2007a). P2X receptors in RVSMCs are involved in mediating tubuloglomerular feedback and sympathetic control of renal vasculature.

Indeed, interstitial ATP has been shown to be an important paracrine agent involved in renal autoregulation. *In vivo* studies demonstrated that elevation of renal perfusion pres-

sure correlated with increased ATP concentration in renal cortical interstitial fluid (Nishiyama *et al*., 2000). These renal interstitial fluid ATP responses to an increase in arterial pressure persisted following the block of L-type voltage-gated calcium channels and correlated with manipulation of the tubuloglomerular feedback response (Nishiyama *et al*., 2001). In line with these observations, Bell and colleagues demonstrated ATP release by apical macula densa cells in response to increase of NaCl concentration in the distal tubular fluid (Bell *et al*., 2003; Komlosi *et al*., 2006). *Ex vivo* studies demonstrated that afferent arteriolar autoregulatory responses were substantially attenuated by selective P2X1 receptor inhibition or desensitization (Inscho *et al*., 2003). Furthermore, it was demonstrated that P2X1 receptor knock-out mice do not exhibit tubuloglomerular feedback (Inscho *et al*., 2003). This evidence suggests that activation of P2X receptors by interstitial ATP mediates renal autoregulatory behaviour. However, tubuloglomerular feedback is largely restricted to regulation of terminal arteriolar resistance, while myogenic mechanism are considered to be the major contributor to autoregulatory resistance adjustments of the afferent arteriole and upstream arterial segments (Cupples and Braam, 2007; Guan *et al*., 2007a). Therefore, the extent to which P2X receptors in RVSMCs from interlobar and arcuate arteries are engaged in mediating purinergic autoregulatory responses is debatable.

On the other hand, opinion about the role of renal sympathetic nerve activity (RSNA) in the regulation of RBF has been revised during the last decade. Indeed, recent experiments on conscious animals in which RSNA was altered using different reflex maneuvers, and in some of which RSNA and RBF were simultaneously measured, revealed that even small changes in RSNA alter RBF (Grady and Bullivant, 1992; Malpas and Evans, 1998; Leonard *et al*., 2000) and that resting RBF increases following renal denervation (Grady and Bullivant, 1992; Malpas and Evans, 1998). Thus, RSNA provides a tonic level of renal vasoconstriction and contributes to control of RBF around normal resting levels (Malpas and Leonard, 2000). Increased RSNA is now recognized as an important cause of the decrease in renal excretory function in hypertension (DiBona and Kopp, 1997; DiBona and Sawin, 2004). One of the possible mechanisms linking increased RSNA to the decrease in renal excretory function is a decrease in RBF and GFR caused by renal vasoconstriction (DiBona, 2004). ATP acting upon P2X receptors is an important sympathetic co-transmitter and putative paracrine agent mediating autoregulatory tubuloglomerular feedback. Our study has identified two important targets in RVSMCs for possible therapeutic intervention: monomeric P2X1 and heteromeric P2X1/4 receptors. Further work will, however, be necessary to examine whether and how these ligand-gated ion channels and their associated signal transduction mechanisms are altered in hypertension.

Acknowledgements

The work was supported by a British Heart Foundation Project Grant PG/08/062/25382 to D.G. and M.H. M.H. is a British Heart Foundation Intermediate Basic Science Research Fellow (FS/06/077). We thank Professor TB Bolton for providing set-up funded by a grant from The Wellcome Trust (042293).

Conflicts of interest

None.

References

Alexander SP, Mathie A, Peters JA (2009). *Guide to Receptors and Channels (GRAC)*, 4th Edition. *Br J Pharmacol* **158** (Suppl 1): S1–S254.

Bao JX, Stjarne L (1993). Dual contractile effects of ATP released by field stimulation revealed by effects of alpha,beta-methylene ATP and suramin in rat tail artery. *Br J Pharmacol* **110**: 1421–1428.

Bell PD, Lapointe JY, Sabirov R, Hayashi S, Peti-Peterdi J, Manabe K *et al*. (2003). Macula densa cell signaling involves ATP release through a maxi anion channel. *Proc Natl Acad Sci U S A* **100**: 4322–4327.

Benham CD, Bolton TB, Lang RJ, Takewaki T (1986). Calcium-activated potassium channels in single smooth muscle cells of rabbit jejunum and guinea-pig mesenteric artery. *J Physiol* **371**: 45–67.

Bo X, Burnstock G (1995). Characterization and autoradiographic localization of [3H] alpha, beta-methylene adenosine 5′-triphosphate binding sites in human urinary bladder. *Br J Urol* **76**: 297–302.

Burnstock G (1972). Purinergic nerves. *Pharmacol Rev* **24**: 509–581.

Cario-Toumaniantz C, Loirand G, Ladoux A, Pacaud P (1998). P2X7 receptor activation-induced contraction and lysis in human saphenous vein smooth muscle. *Circ Res* **83**: 196–203.

Chan CM, Unwin RJ, Bardini M, Oglesby IB, Ford AP, Townsend-Nicholson A *et al*. (1998). Localization of P2X1 purinoceptors by autoradiography and immunohistochemistry in rat kidneys. *Am J Physiol* **274**: F799–F804.

Cupples WA, Braam B (2007). Assessment of renal autoregulation. *Am J Physiol Renal Physiol* **292**: F1105–F1123.

Damer S, Niebel B, Czeche S, Nickel P, Ardanuy U, Schmalzing G *et al*. (1998). NF279: a novel potent and selective antagonist of P2X receptor-mediated responses. *Eur J Pharmacol* **350**: R5–R6.

DiBona GF (2004). The sympathetic nervous system and hypertension: recent developments. *Hypertension* **43**: 147–150.

DiBona GF, Kopp UC (1997). Neural control of renal function. *Physiol Rev* **77**: 75–197.

DiBona GF, Sawin LL (2004). Effect of renal denervation on dynamic autoregulation of renal blood flow. *Am J Physiol Renal Physiol* **286**: F1209–F1218.

Evans RJ, Surprenant A (1992). Vasoconstriction of guinea-pig submucosal arterioles following sympathetic nerve stimulation is mediated by the release of ATP. *Br J Pharmacol* **106**: 242–249.

Evans RJ, Lewis C, Buell G, Valera S, North RA, Surprenant A (1995). Pharmacological characterization of heterologously expressed ATP-gated cation channels (P2x purinoceptors). *Mol Pharmacol* **48**: 178–183.

Evans RJ, Lewis C, Virginio C, Lundstrom K, Buell G, Surprenant A *et al*. (1996). Ionic permeability of, and divalent cation effects on, two ATP-gated cation channels (P2X receptors) expressed in mammalian cells. *J Physiol* **497** (Pt 2): 413–422.

Galligan JJ, Herring A, Harpstead T (1995). Pharmacological characterization of purinoceptor-mediated constriction of submucosal arterioles in guinea pig ileum. *J Pharmacol Exp Ther* **274**: 1425–1430.

Gerdes J, Li L, Schlueter C, Duchrow M, Wohlenberg C, Gerlach C *et al*. (1991). Immunobiochemical and molecular biologic characterization of the cell proliferation-associated nuclear antigen that is defined by monoclonal antibody Ki-67. *Am J Pathol* **138**: 867–873.

Gordienko DV, Clausen C, Goligorsky MS (1994). Ionic currents and endothelin signaling in smooth muscle cells from rat renal resistance arteries. *Am J Physiol* **266**: F325–F341.

Grady HC, Bullivant EM (1992). Renal blood flow varies during normal activity in conscious unrestrained rats. *Am J Physiol* **262**: R926–R932.

Guan Z, Osmond DA, Inscho EW (2007a). P2X receptors as regulators of the renal microvasculature. *Trends Pharmacol Sci* **28**: 646–652.

Guan Z, Osmond DA, Inscho EW (2007b). Purinoceptors in the kidney. *Exp Biol Med (Maywood)* **232**: 715–726.

Harhun MI, Gordienko DV, Povstyan OV, Moss RF, Bolton TB (2004). Function of interstitial cells of cajal in the rabbit portal vein. *Circ Res* **95**: 619–626.

Harhun M, Gordienko D, Kryshtal D, Pucovsky V, Bolton T (2006). Role of intracellular stores in the regulation of rhythmical $[Ca^{2+}]_i$ changes in interstitial cells of Cajal from rabbit portal vein. *Cell Calcium* **40**: 287–298.

Harhun M, Povstyan O, Gordienko D (2009). P2X Receptor-mediated current in myocytes from renal resistance arteries. *J General Physiology* **134**: 17.

Hughes S, Chan-Ling T (2004). Characterization of smooth muscle cell and pericyte differentiation in the rat retina *in vivo*. *Invest Ophthalmol Vis Sci* **45**: 2795–2806.

Hulsmann M, Nickel P, Kassack M, Schmalzing G, Lambrecht G, Markwardt F (2003). NF449, a novel picomolar potency antagonist at human P2X1 receptors. *Eur J Pharmacol* **470**: 1–7.

Inscho EW, Cook AK, Imig JD, Vial C, Evans RJ (2003). Physiological role for P2X1 receptors in renal microvascular autoregulatory behavior. *J Clin Invest* **112**: 1895–1905.

Khakh BS, Proctor WR, Dunwiddie TV, Labarca C, Lester HA (1999). Allosteric control of gating and kinetics at P2X(4) receptor channels. *J Neurosci* **19**: 7289–7299.

Komlosi P, Fintha A, Bell PD (2006). Unraveling the relationship between macula densa cell volume and luminal solute concentration/osmolality. *Kidney Int* **70**: 865–871.

Le KT, Babinski K, Seguela P (1998). Central P2X4 and P2X6 channel subunits coassemble into a novel heteromeric ATP receptor. *J Neurosci* **18**: 7152–7159.

Leonard BL, Navakatikyan MA, Malpas SC (2000). Differential regulation of the oscillations in sympathetic nerve activity and renal blood flow following volume expansion. *Auton Neurosci* **83**: 19–28.

Lewis CJ, Evans RJ (2000). Lack of run-down of smooth muscle P2X receptor currents recorded with the amphotericin permeabilized patch technique, physiological and pharmacological characterization of the properties of mesenteric artery P2X receptor ion channels. *Br J Pharmacol* **131**: 1659–1666.

Lewis CJ, Evans RJ (2001). P2X receptor immunoreactivity in different arteries from the femoral, pulmonary, cerebral, coronary and renal circulations. *J Vasc Res* **38**: 332–340.

Loirand G, Pacaud P (1995). Mechanism of the ATP-induced rise in cytosolic Ca2+ in freshly isolated smooth muscle cells from human saphenous vein. *Pflugers Arch* **430**: 429–436.

McLaren GJ, Sneddon P, Kennedy C (1998). Comparison of the actions of ATP and UTP and P(2X1) receptors in smooth muscle of the rat tail artery. *Eur J Pharmacol* **351**: 139–144.

Malpas SC, Evans RG (1998). Do different levels and patterns of sympathetic activation all provoke renal vasoconstriction?*J Auton Nerv Syst* **69**: 72–82.

Malpas SC, Leonard BL (2000). Neural regulation of renal blood flow: a re-examination. *Clin Exp Pharmacol Physiol* **27**: 956–964.

Nicke A, Kerschensteiner D, Soto F (2005). Biochemical and functional evidence for heteromeric assembly of P2X1 and P2X4 subunits. *J Neurochem* **92**: 925–933.

Nishiyama A, Navar LG (2002). ATP mediates tubuloglomerular feedback. *Am J Physiol Regul Integr Comp Physiol* **283**: R273–R275.

Nishiyama A, Majid DS, Taher KA, Miyatake A, Navar LG (2000). Relation between renal interstitial ATP concentrations and autoregulation-mediated changes in renal vascular resistance. *Circ Res* **86**: 656–662.

Nishiyama A, Majid DS, Walker M, III, Miyatake A, Navar LG (2001). Renal interstitial atp responses to changes in arterial pressure during alterations in tubuloglomerular feedback activity. *Hypertension* **37**: 753–759.

Nori S, Fumagalli L, Bo X, Bogdanov Y, Burnstock G (1998). Coexpression of mRNAs for P2X1, P2X2 and P2X4 receptors in rat vascular smooth muscle: an *in situ* hybridization and RT–PCR study. *J Vasc Res* **35**: 179–185.

North RA (2002). Molecular physiology of P2X receptors. *Physiol Rev* **82**: 1013–1067.

North RA, Verkhratsky A (2006). Purinergic transmission in the central nervous system. *Pflugers Arch* **452**: 479–485.

Ralevic V (2009). Purines as neurotransmitters and neuromodulators in blood vessels. *Curr Vasc Pharmacol* **7**: 3–14.

Ralevic V, Burnstock G (1991). Roles of P2-purinoceptors in the cardiovascular system. *Circulation* **84**: 1–14.

Rettinger J, Schmalzing G, Damer S, Muller G, Nickel P, Lambrecht G (2000). The suramin analogue NF279 is a novel and potent antagonist selective for the P2X(1) receptor. *Neuropharmacology* **39**: 2044–2053.

Rettinger J, Braun K, Hochmann H, Kassack MU, Ullmann H, Nickel P *et al*. (2005). Profiling at recombinant homomeric and heteromeric rat P2X receptors identifies the suramin analogue NF449 as a highly potent P2X1 receptor antagonist. *Neuropharmacology* **48**: 461–468.

Stehno-Bittel L, Sturek M (1992). Spontaneous sarcoplasmic reticulum calcium release and extrusion from bovine, not porcine, coronary artery smooth muscle. *J Physiol* **451**: 49–78.

Surprenant A, North RA (2009). Signaling at purinergic P2X receptors. *Annu Rev Physiol* **71**: 333–359.

Torres GE, Egan TM, Voigt MM (1999). Hetero-oligomeric assembly of P2X receptor subunits. Specificities exist with regard to possible partners. *J Biol Chem* **274**: 6653–6659.

Turner CM, Vonend O, Chan C, Burnstock G, Unwin RJ (2003). The pattern of distribution of selected ATP-sensitive P2 receptor subtypes in normal rat kidney: an immunohistological study. *Cells Tissues Organs* **175**: 105–117.

Valera S, Hussy N, Evans RJ, Adami N, North RA, Surprenant A *et al*. (1994). A new class of ligand-gated ion channel defined by P2x receptor for extracellular ATP. *Nature* **371**: 516–519.

Vanderwinden JM, Rumessen JJ, De Laet MH, Vanderhaeghen JJ, Schiffmann SN (1999). CD34+ cells in human intestine are fibroblasts adjacent to, but distinct from, interstitial cells of Cajal. *Lab Invest* **79**: 59–65.

Walsh MP (1994). Regulation of vascular smooth muscle tone. *Can J Physiol Pharmacol* **72**: 919–936.

Wier WG, Zang WJ, Lamont C, Raina H (2009). Sympathetic neurogenic Ca^{2+} signalling in rat arteries: ATP, noradrenaline and neuropeptide Y. *Exp Physiol* **94**: 31–37.

Wilkinson KD, Lee KM, Deshpande S, Duerksen-Hughes P, Boss JM, Pohl J (1989). The neuron-specific protein PGP 9.5 is a ubiquitin carboxyl-terminal hydrolase. *Science* **246**: 670–673.

Yoshida T, Owens GK (2005). Molecular determinants of vascular smooth muscle cell diversity. *Circ Res* **96**: 280–291.